**Applied Mathematics, 2014, 5, 1913-1926**
Published Online July 2014 in SciRes. http://www.scirp.org/journal/am
http://dx.doi.org/10.4236/am.2014.513185

Scientific Research

# Mathematical Analysis of a Large Scale Vector SIS Malaria Model in a Patchy Environment

**Josephine Wairimu[1,2*], Sallet Gauthier[2], Wandera Ogana[1]**

[1]School of Mathematics, University of Nairobi, Nairobi, Kenya
[2]INRIA, Metz and University of Lorraine, Lorraine, France
Email: jwndirangu@uonbi.ac.ke

Received 20 April 2014; revised 26 May 2014; accepted 3 June 2014



## Abstract

**We answer the stability question of the large scale SIS model describing transmission of highland malaria in Western Kenya in a patchy environment, formulated in [1]. There are two equilibrium states and their stability depends on the basic reproduction number, $\mathcal{R}_0$ [2]. If $\mathcal{R}_0 \le 1$, the disease-free steady solution is globally asymptotically stable and the disease always dies out. If $\mathcal{R}_0 > 1$, there exists a unique endemic equilibrium which is globally stable and the disease persists. Application is done on data from Western Kenya. The age structure reduces the level of infection and the populations settle to the equilibrium faster than in the model without age structure.**

## Keywords

**Highland Malaria, Differentiated Susceptibility and Infectivity, Monotone Dynamical Systems**

## 1. Introduction

We recall the large scale system developed in [1] reduced into a compact form as

$$\dot{X} = \mathcal{A}\,\mathrm{diag}\left(1-X\right)\mathcal{B}X + \left(-\mathcal{C} + \tilde{\mathcal{M}}\right)X \tag{1}$$

where
$X = (x, y, z)$, is a vector representing; $x$ is the proportion of infectious children, $y$ is the proportion of infectious adults, and $z$ is the proportion of infectious mosquitoes.

*Corresponding author.

**How to cite this paper:** Wairimu, J., Gauthier, S. and Ogana, W. (2014) Mathematical Analysis of a Large Scale Vector SIS Malaria Model in a Patchy Environment. *Applied Mathematics*, **5**, 1913-1926. http://dx.doi.org/10.4236/am.2014.513185

$\mathcal{A}$, $\mathcal{B}$ and the matrix $\mathcal{C}$ are the matrices.

$$\mathcal{A}=\begin{pmatrix}\operatorname{diag}\left(\beta_1^C\right)\operatorname{diag}\left(\bar{N}\right)^{-1}\operatorname{diag}\left(\bar{V}\right) & 0 & 0\\ 0 & \operatorname{diag}\left(\beta_1^A\right)\operatorname{diag}\left(\bar{N}\right)^{-1}\operatorname{diag}\left(\bar{V}\right) & 0\\ 0 & 0 & \operatorname{diag}\left(\bar{N}\right)^{-1}\end{pmatrix}$$

$$\mathcal{B}=\begin{pmatrix}0 & 0 & I_n\\ 0 & 0 & I_n\\ \operatorname{diag}\left(\beta_2^C\right)\operatorname{diag}\left(\bar{N}^C\right) & \operatorname{diag}\left(\beta_2^A\right)\operatorname{diag}\left(\bar{N}^A\right) & 0\end{pmatrix}$$

$$\mathcal{C}=\begin{pmatrix}\operatorname{diag}\left(\gamma^C+\nu.1+\mu_h^C\right) & 0 & 0\\ -\nu I_n & \operatorname{diag}\left(\gamma^A+\mu_h^A\right) & 0\\ 0 & 0 & \operatorname{diag}\left(\mu_v\right)\end{pmatrix}$$

$$\tilde{\mathcal{M}}=\begin{pmatrix}\tilde{M}^C & 0 & 0\\ 0 & \tilde{M}^A & 0\\ 0 & 0 & \tilde{M}^v\end{pmatrix}$$

The authors used the preceding matrices and the vector $X=(x,y,z)$ to rewrite Equation (10) in [1] in a compact form as

$$X'=\mathcal{A}\operatorname{diag}(1-X)\mathcal{B}X+\left(-\mathcal{C}+\tilde{\mathcal{M}}\right)X. \tag{2}$$

This system evolves on the unit cube of $\mathbb{R}^{3n}$.

## Calculation of the Basic Reproduction Number

We use the classical framework defined in [3] [4].

The application $\mathcal{F}(x)=\mathcal{A}\operatorname{diag}(1-X)\mathcal{B}X$ represents the rate of appearance of new infections in the compartments in the patches.

The function $\mathcal{V}(X)=\left(-\mathcal{C}+\tilde{\mathcal{M}}\right)X$ is the rate of transfer of individuals in compartments.

If $\mathcal{F}(x)$ is set to zero, system becomes $\dot{X}=\left(-\mathcal{C}+\tilde{\mathcal{M}}\right)X$, which is a linear system, and we have already seen that $\left(-\mathcal{C}+\tilde{\mathcal{M}}\right)$ is a stable Metzler matrix.

**Proposition 1.1**

The basic reproduction number of system (1) is

$$\mathcal{R}_0=\rho\left(-\left(-\mathcal{C}+\tilde{\mathcal{M}}\right)^{-1}\mathcal{A}\mathcal{B}\right).$$

**Proof**

This is straightforward since the Jacobian of $\mathcal{F}$ computed at the DFE $X=0$ is

$$F=\mathcal{A}\mathcal{B},$$

and the Jacobian of $\mathcal{V}(X)$ computed at the DFE is $\mathfrak{V}=\left(-\mathcal{C}+\tilde{\mathcal{M}}\right)$.

The next generation matrix is then $K=-\left(-\mathcal{C}+\tilde{\mathcal{M}}\right)^{-1}\mathcal{A}\mathcal{B}$ □

We can develop the expression of $\mathcal{R}_0$ further:

$$F=\mathcal{A}\mathcal{B}=\begin{pmatrix}0 & 0 & \operatorname{diag}\left(\beta_1^C\right)\operatorname{diag}\left(\bar{N}\right)^{-1}\operatorname{diag}\left(\bar{V}\right)\\ 0 & 0 & \operatorname{diag}\left(\beta_1^A\right)\operatorname{diag}\left(\bar{N}\right)^{-1}\operatorname{diag}\left(\bar{V}\right)\\ \operatorname{diag}\left(\mu_v\right)\operatorname{diag}\left(\beta_2^C\right)\operatorname{diag}\left(\bar{N}^C\right) & \operatorname{diag}\left(\mu_v\right)\operatorname{diag}\left(\beta_2^A\right)\operatorname{diag}\left(\bar{N}^A\right) & 0\end{pmatrix} \tag{3}$$

$$\mathfrak{V}=\left(-\mathcal{C}+\tilde{\mathcal{M}}\right)=\begin{pmatrix}-\operatorname{diag}\left(\gamma+\nu 1+\mu_h^C\right)+\tilde{M}^C & 0 & 0\\ \nu I_n & -\operatorname{diag}\left(\gamma+\mu_h^A\right)+\tilde{M}^A & 0\\ 0 & 0 & -\operatorname{diag}\left(\mu_v\right)+\tilde{M}^v\end{pmatrix} \tag{4}$$

Then we can compute the nonnegative matrix $-\mathfrak{V}^{-1}$, which is a lower triangular matrix

$$-\mathfrak{V}^{-1}=\begin{pmatrix}V_{11}^- & 0 & 0\\ V_{21}^- & V_{22}^- & 0\\ 0 & 0 & V_{33}^-\end{pmatrix}$$

with

$$V_{11}^-=-\left(-\operatorname{diag}\left(\gamma+\nu.1+\mu_h^C\right)+\tilde{M}^C\right)^{-1}$$

$$V_{21}^-=\nu\left(-\operatorname{diag}\left(\gamma+\mu_h^A\right)+\tilde{M}^A\right)^{-1}\left(-\operatorname{diag}\left(\gamma+\nu.1+\mu_h^C\right)+\tilde{M}^C\right)^{-1}$$

$$V_{22}^-=-\left(-\operatorname{diag}\left(\gamma+\mu_h^A\right)+\tilde{M}^A\right)^{-1}$$

$$V_{33}^-=-\left(-\operatorname{diag}\left(\mu_v\right)+\tilde{M}^v\right)^{-1}$$

The next generation matrix is a block matrix

$$K=\begin{pmatrix}0 & 0 & K_{13}\\ 0 & 0 & K_{23}\\ K_{31} & K_{32} & 0\end{pmatrix},$$

with

$$K_{13}=-\operatorname{diag}\left(\beta_1^C\right)\operatorname{diag}\left(\bar{N}\right)^{-1}\operatorname{diag}\left(\bar{V}\right)\left(-\operatorname{diag}\left(\mu_v\right)+\tilde{M}^v\right)^{-1}$$

$$K_{23}=-\operatorname{diag}\left(\beta_1^A\right)\operatorname{diag}\left(\bar{N}\right)^{-1}\operatorname{diag}\left(\bar{V}\right)\left(-\operatorname{diag}\left(\mu_v\right)+\tilde{M}^v\right)^{-1}$$

$$K_{31}=-\operatorname{diag}\left(\mu_v\right)\operatorname{diag}\left(\beta_2^C\right)\operatorname{diag}\left(\bar{N}^C\right)\left(-\operatorname{diag}\left(\gamma+\nu.1+\mu_h^C\right)+\tilde{M}^C\right)^{-1}$$

$$+\nu\operatorname{diag}\left(\mu_v\right)\operatorname{diag}\left(\beta_2^A\right)\operatorname{diag}\left(\bar{N}^A\right)\left(-\operatorname{diag}\left(\gamma+\mu_h^A\right)+\tilde{M}^A\right)^{-1}\left(-\operatorname{diag}\left(\gamma+\nu.1+\mu_h^C\right)+\tilde{M}^C\right)^{-1}$$

$$K_{32}=-\operatorname{diag}\left(\mu_v\right)\operatorname{diag}\left(\beta_2^A\right)\operatorname{diag}\left(\bar{N}^A\right)\left(-\operatorname{diag}\left(\gamma+\mu_h^A\right)+\tilde{M}^A\right)^{-1}$$

The block structure of $K$ implies (see [4]) that

$$\mathcal{R}_0^2=\rho\left(K_{31}K_{13}+K_{32}K_{23}\right)$$

When $\mathcal{R}_0<1$, the DFE is locally asymptotically stable, and if $\mathcal{R}_0>1$ the DFE is unstable, see [3] [4].

## 2. Main Result

In this section we establish a global stability result for the DFE when $\mathcal{R}_0\le 1$ and a global stability result when $\mathcal{R}_0>1$. We have the following theorem

**Theorem 2.1**

We consider the system (1) with the matrix $M^C+M^A+M^v$ irreducible.

Then

If $\mathcal{R}_0\le 1$, then the system (1) is globally asymptotically stable at the origin

If $\mathcal{R}_0>1$, then there exists a unique endemic equilibrium $X^*$, which is globally asymptotically stable on $\mathfrak{K}\in[0,1]^{3n}$.

**Proof**

We recall system (1),

$$\dot{X} = \mathcal{A}\operatorname{diag}(1-X)\mathcal{B}X + \left[-\mathcal{C} + \tilde{\mathcal{M}}\right]X$$

The Jacobian at the origin will be given by

$$J(X) = \mathcal{A}\operatorname{diag}(1-X)\mathcal{B} - \mathcal{A}\operatorname{diag}(\mathcal{B}X) + \left[-\mathcal{C} + \tilde{\mathcal{M}}\right]$$

and

$$J(0) = \mathcal{A}\mathcal{B} + \left[-\mathcal{C} + \tilde{\mathcal{M}}\right].$$

To prove the first part of the proposition above we assume that $\mathcal{R}_0 \le 1$ Following [5], $A = B + C$ is a regular splitting of $A$ if $B$ is Metzler stable and $C \ge 0$. Thus in our case $\left[-\mathcal{C} + \tilde{\mathcal{M}}\right]$ has to be a stable Metzler matrix which is invertible and $\mathcal{A}\mathcal{B} \ge 0$, or equivalently, $\left[-\mathcal{C} + \tilde{\mathcal{M}}\right]$ has to be an M-matrix.

We know from Thieme [6], Driessche [4], and Varga [7] that

$$\mathcal{R}_0 \le 1 \iff s\left(-\mathcal{A}\mathcal{B} + \left[-\mathcal{C} + \tilde{\mathcal{M}}\right]^{-1}\right) \le 0.$$

From the preceding section we know that the Jacobian $J$ is an irreducible Metzler matrix. So, by Perron-Frobenius, there exists a positive vector $\mathbf{c} \gg 0$, such that

$$\left(\mathcal{A}\mathcal{B} - \mathcal{C} + \tilde{\mathcal{M}}\right)^T \mathbf{c} = s(J(0))\mathbf{c} \le 0.$$

To prove the global stability of the DFE we consider the Lyapunov function

$$L(X) = \langle \mathbf{c} | X \rangle,$$

where $\langle | \rangle$, denotes the inner product. From the definition of $\mathbf{c} \gg 0$, this function is actually positive definite in the nonnegative orthant.

We compute the derivative of $L$ along the trajectories of (1) and find that it is equivalent to

$$\begin{aligned} L'(X) &= \left\langle \mathbf{c} \middle| \mathcal{A}\operatorname{diag}(1-X)\mathcal{B} + \left[-\mathcal{C} + \tilde{\mathcal{M}}\right]X \right\rangle \le \left\langle \mathbf{c} \middle| \left(\mathcal{A}\mathcal{B} + \left[-\mathcal{C} + \tilde{\mathcal{M}}\right]\right)X \right\rangle \\ &= \left\langle \left(\mathcal{A}\mathcal{B} + \left[-\mathcal{C} + \tilde{\mathcal{M}}\right]\right)^T \mathbf{c} \middle| X \right\rangle = \left\langle s(J(0))\mathbf{c} \middle| X \right\rangle = s(J(0))\langle \mathbf{c} | X \rangle \le 0, \end{aligned} \tag{5}$$

We see that $0 \le X \le 1$, it is clear that $(1-X)B \le XB$, hence the above inequality.

Since $s(J(0)) \le 0$ the derivative is non positive. The DFE is stable.

We will prove the asymptotic stability when $\mathcal{R}_0 \le 1$.

First we consider the case when $\mathcal{R}_0 < 1$. Since we know that $\mathcal{R}_0 < 1$ implies $s(J) < 0$, $L'$ is negative definite, since $\mathbf{c} \gg 0$. This proves the asymptotic stability of the DFE.

When $\mathcal{R}_0 = 1$, we consider the largest invariant set contained in the set

$$\mathcal{L} = \{X \mid L'(X) = 0\}.$$

For such an $X$ we have

$$0 = \left\langle \mathbf{c} \middle| \mathcal{A}\operatorname{diag}(1-X)\mathcal{B}X + \left[-\mathcal{C} + \tilde{\mathcal{M}}\right]X \right\rangle = \left\langle \mathbf{c} \middle| \left(\mathcal{A}\mathcal{B} + \left[-\mathcal{C} + \tilde{\mathcal{M}}\right]\right)X - \mathcal{A}\operatorname{diag}(X)\mathcal{B}X \right\rangle,$$

but since $L'(x) = 0$, we have by the inequality (5),

$$\left\langle \mathbf{c} \middle| \left(\mathcal{A}\mathcal{B} + \left[-\mathcal{C} + \tilde{\mathcal{M}}\right]\right)X \right\rangle = 0.$$

Hence

$$V'(X) = -\langle \mathbf{c} | \mathcal{A}\operatorname{diag}(X)\mathcal{B}X \rangle.$$

Since $\mathbf{c} \gg 0$ then $\mathcal{A}\operatorname{diag}(X)\mathcal{B}X = 0$ or equivalently $\operatorname{diag}(X)\mathcal{B}X = 0$

Now we show that the largest invariant set in $\mathcal{L}$ is reduced to the origin.

$$\operatorname{diag}(X)\mathcal{B}X=\begin{pmatrix}\operatorname{diag}(x)z\\ \operatorname{diag}(y)z\\ \operatorname{diag}(z)\left(\operatorname{diag}\left(\beta_2^C\right)\operatorname{diag}\left(\bar{N}^C\right)x+\operatorname{diag}\left(\beta_2^A\right)\operatorname{diag}\left(\bar{N}^A\right)y\right)\end{pmatrix}$$

We must have, for any index $i$, $x_i z_i = 0$ and $y_i z_i = 0$

Suppose $x_i = 0$ since

$$x_i' = \beta_{1i}^C \frac{\bar{V}_i}{\bar{N}_i} z_i (1-x_i) - \left(\gamma_i^C + \mu_{h,i}^C + \nu\right) x_i + \sum_{j=1, j\neq i}^{n} m_{ij}^C \frac{\bar{N}_j^C}{\bar{N}_i^C} x_j - x_i \sum_{j=1, j\neq i}^{n} m_{ji}^C$$

we have

$$x_i' = \beta_{1i}^C \frac{\bar{V}_i}{\bar{N}_i} z_i + \sum_{j=1, j\neq i}^{n} m_{ij}^C \frac{\bar{N}_j^C}{\bar{N}_i^C} x_j = 0.$$

Then $z_i = 0$ and $x_j = 0$ for any patch $j$, with a "children" arc leaving $j$ and entering $i$.

Since $z_i = 0$ and $x_i = 0$ and since

$$z_i' = \beta_{2i}^C \frac{\bar{N}_i^C}{\bar{N}_i} x_i (1-z_i) + \beta_{2i}^A \frac{\bar{N}_i^A}{\bar{N}_i} y_i (1-z_i) - \mu_{v,i} z_i + \sum_{j=1, j\neq i}^{n} m_{ij}^v \frac{\bar{V}_j}{\bar{V}_i} z_j - z_i \sum_{j=1, j\neq i}^{n} m_{ji}^v$$

we have

$$z_i' = \beta_{2i}^A \frac{\bar{N}_i^A}{\bar{N}_i} y_i + \sum_{j=1, j\neq i}^{n} m_{ij}^v \frac{\bar{V}_j}{\bar{V}_i} z_j = 0$$

Again $y_i = 0$ and $z_j = 0$ for any patch $j$ with a "mosquito" arc leaving $j$ and entering $i$.

Now $x_i = y_i = z_i = 0$ implies

$$y_i' = \sum_{j=1, j\neq i}^{n} m_{ij} \frac{N_j^A}{N_i^A} y_j$$

which implies that $y_j = 0$ for any patch with a "adult" arc leaving $j$ and entering $i$.

Now, since any patch can be reached by a path composed of "children", "adult" or "mosquito" arcs, this proves that $x_i = y_i = z_i = 0$ for any index.

This ends the proof for the global asymptotic stability of the DFE from LaSalle's Invariance Principle [8].

To prove the second part of our theorem, when $\mathcal{R}_0 > 1$, we need the following theorem from [9].

**Theorem 2.2**

Let $F$ be a $C^1$ vector field in $\mathbb{R}^n$, whose flow $\phi$ preserves $\mathbb{R}_+^n$ for $t \geq 0$ and is strongly monotone in $\mathbb{R}_+^n$. Assume that the origin is an equilibrium and that all trajectories in $\mathbb{R}_+^n$ are bounded. Suppose the matrix-valued map $DF : \mathbb{R}_+^n \to \mathbb{R}_+^n \times \mathbb{R}_+^n$ is strictly anti monotone, in the sense that,

$$\text{if } x < y, \text{ then } DF(x) > DF(y),$$

then either all the trajectories in $\mathbb{R}_+^n \setminus \{0\}$ tend to the origin, or else there is a unique equilibrium $p \in Int\, \mathbb{R}_+^n \ (p \gg 0)$ and all the trajectories in $\mathbb{R}_+^n$ tend to $p$.

For our case we shall consider the positively invariant set $[0,1]^{3n}$, which is diffeomorphic to the nonnegative orthant $\mathbb{R}_+^{3n}$. Since the faces of the cube of type $x_i = 1$ are repulsive for the vector field associated to (1), all the trajectories are bounded in $[0,1]^{3n}$.

We recall system 1.

$$X' = \mathcal{A}\operatorname{diag}(1-X)\mathcal{B}X + \left(-\mathcal{C} + \tilde{\mathcal{M}}\right)X$$

If we take $X_1 < X_2 \in X$, then

$$F(X_1) = \mathcal{A}\operatorname{diag}(1-X_1)(\mathcal{B}X_1) + \left[-\mathcal{C} + \tilde{\mathcal{M}}\right]X_1$$

$$F(X_2) = \mathcal{A}\operatorname{diag}(1-X_2)(\mathcal{B}X_2) + \left[-\mathcal{C} + \tilde{\mathcal{M}}\right]X_2$$

Clearly

$$\left[-\mathcal{C}+\tilde{\mathcal{M}}\right]X_1<\left[-\mathcal{C}+\tilde{\mathcal{M}}\right]X_2,$$

since the quantities are positive.

Now we prove that

$$\mathcal{A}\text{diag}\left(1-X_1\right)\left(\mathcal{B}X_1\right)<\mathcal{A}\text{diag}\left(1-X_2\right)\left(\mathcal{B}X_2\right)$$

and hence show that the system is strongly monotone. That is

$$\mathcal{A}\text{diag}\left(\mathcal{B}X_1\right)-\mathcal{A}\text{diag}\left(X_1\right)\mathcal{B}X_1<\mathcal{A}\text{diag}\left(X_2\right)-\mathcal{A}\text{diag}\left(X_2\right)\mathcal{B}X_2$$

or

$$-\mathcal{A}\text{diag}\left(X_1\right)\mathcal{B}X_1<-\mathcal{A}\text{diag}\left(X_2\right)\mathcal{B}X_2.$$

Considering the structure of $\mathcal{A}$ and $\mathcal{B}$ and having $X_1<X_2$ in $[0,1]^{3n}$ and the fact that a sign change reverses the inequality, then

$$\mathcal{A}\text{diag}\left(X_1\right)\mathcal{B}X_1>\mathcal{A}\text{diag}\left(X_2\right)\mathcal{B}X_2$$

hence

$$-\mathcal{A}\text{diag}\left(X_1\right)\mathcal{B}X_1<-\mathcal{A}\text{diag}\left(X_2\right)\mathcal{B}X_2.$$

To prove that theorem, we recall the Jacobian $J\left(X\right)$ of system (1)

$$J(X)=-\mathcal{A}\text{diag}\left(\mathcal{B}X\right)+\mathcal{A}\text{diag}\left(1-X\right)\mathcal{B}+\left[-\mathcal{C}+\tilde{\mathcal{M}}\right],$$

Again for any $X_1<X_2\in X$ , then $\text{diag}\left(1-X_2\right)<\text{diag}\left(1-X_1\right)$. Since the matrix $\mathcal{B}$ has on each row a positive term, since $\mathcal{A}$ is a diagonal matrix with positive terms, we deduce

$$\mathcal{A}\text{diag}\left(1-X_2\right)\mathcal{B}<\mathcal{A}\text{diag}\left(1-X_1\right)\mathcal{B}$$

Considering the structure of $\mathcal{B}$ we have, if $X_1<X_2$, the relation $\mathcal{B}X_1<\mathcal{B}X_2$ holds and consequently $-\mathcal{A}\text{diag}\left(\mathcal{B}X_2\right)<-\mathcal{A}\text{diag}\left(\mathcal{B}X_1\right)$.

Finally we have $J\left(X_2\right)<J\left(X_1\right)$, therefore the anti monotone criteria is met.

We will prove that no trajectory tends to the origin.

We have $\mathcal{R}_0>1$ which is equivalent to $s\left(J\left(0\right)\right)>1$. Then there exists a positive vector $\mathbf{c}\gg 0$ such that

$$J\left(0\right)^T\mathbf{c}=\left(\mathcal{A}\mathcal{B}-\mathcal{C}+\tilde{\mathcal{M}}\right)^T\mathbf{c}=s\left(J\left(0\right)\right)\mathbf{c}.$$

We consider the Chetaev function on a neighborhood of the origin

$$V\left(X\right)=\left\langle\mathbf{c}\middle|X\right\rangle.$$

An simple computation gives

$$V'\left(X\right)=\left\langle\mathbf{c}\middle|\left[s\left(J\left(o\right)\right)I_n-\mathcal{A}\text{diag}\left(X\right)\mathcal{B}\right]X\right\rangle.$$

Then in a sufficiently small neighborhood of the origin, in $[0,1]^{3n}$, $V'\left(X\right)>0$. This proves that for $\varepsilon>0$ sufficiently small, the hyperplane $\left\{X\middle|\left\langle\mathbf{c}\middle|X\right\rangle=\varepsilon\right\}$ is a barrier for the vector field associated to (1). This proves that no trajectory tends to the origin. Then we conclude, by Hirsch theorem, the existence of an attractive endemic equilibrium $X^*$ in the interior of the cube.

To prove stability, we shall compute $J\left(X^*\right)X^*$:

$$J\left(X^*\right)X^*=-\mathcal{A}\text{diag}\left(\mathcal{B}X^*\right)X^*+\mathcal{A}\text{diag}\left(1-X^*\right)\mathcal{B}X^*+\left[-\mathcal{C}+\tilde{\mathcal{M}}\right]X^*.$$

Taking into account that $X^*$ is an equilibrium gives

$$\mathcal{A}\text{diag}\left(1-X^*\right)\mathcal{B}X^*+\left(-\mathcal{C}+\tilde{\mathcal{M}}\right)X^*=0,$$

therefore

$$J\left(X^*\right)X^* = -\mathcal{A}\mathrm{diag}\left(\mathcal{B}X^*\right)X^* \ll 0$$

since $X^* \gg 0$.

We have proved that there exists a vector $X^* \gg 0.$ such that for the Metzler matrix $J\left(X^*\right)$ we have $J\left(X^*\right)X^* \ll 0$. This implies that $J\left(X^*\right)$ is Hurwitz [10] [11].

This completes the proof of the global asymptotic stability of the endemic equilibrium.

## 3. An Example in Two Patches

In this section we give a result to the case of two patches. We shall use the structure defined in Subsection 1.1.

$$\mathcal{F} = \begin{pmatrix} \beta_{11}^C I_{v,1}\dfrac{\left(N_1^C - I_{h,1}^C\right)}{N_1} \\ \beta_{12}^C I_{v,2}\dfrac{\left(N_2^C - I_{h,2}^C\right)}{N_2} \\ \beta_{11}^A I_{v,1}\dfrac{\left(N_1^A - I_{h,1}^A\right)}{N_1} \\ \beta_{12}^A I_{v,2}\dfrac{\left(N_2^A - I_{h,2}^A\right)}{N_2} \\ \dfrac{\left(V_1 - I_{v,1}\right)}{N_1}\left(\beta_{21}^C I_{h,1}^C + \beta_{21}^A I_{h,1}^A\right) \\ \dfrac{\left(V_2 - I_{v,2}\right)}{N_2}\left(\beta_{22}^C I_{h,2}^C + \beta_{22}^A I_{h,2}^A\right) \end{pmatrix}, \quad \mathcal{V} = \begin{pmatrix} -\left(\gamma_1^C + \mu_1^C + \nu\right)I_{h,1}^C + m_{12}^c I_{h,2}^C - m_{21}^c I_{h,1}^C \\ -\left(\gamma_2^C + \mu_2^C + \nu\right)I_{h,2}^C + m_{21}^c I_{h,1}^C - m_{12}^c I_{h,2}^C \\ -\left(\gamma_1^A + \mu_1^A\right)I_{h,1}^A + m_{12}^A I_{h,2}^A - m_{21}^A I_{h,1}^A \\ -\left(\gamma_2^A + \mu_2^A\right)I_{h,2}^A + m_{21}^A I_{h,2}^A - m_{12}^A I_{h,1}^A \\ -\mu_v I_{v,1} + m_{12}^v I_{v,2} - m_{21}^v I_{v,1} \\ -\mu_v I_{v,2} + m_{21}^v I_{v,1} - m_{12}^v I_{v,2} \end{pmatrix}.$$

The basic reproduction number is given by $\rho\left(-FV^{-1}\right)$ From our example and at the DFE, this matrix is defined by $FV^{-1}$

which has the values

$$\begin{pmatrix} 0 & 0 & 0 & 0 & \dfrac{\beta_{11}^C N_1^C}{\mu_v N_1} & 0 \\ 0 & 0 & 0 & 0 & 0 & \dfrac{\beta_{12}^C N_2^C}{\mu_v N_2} \\ 0 & 0 & 0 & 0 & \dfrac{\beta_{11}^A N_1^A}{\mu_v N_1} & 0 \\ 0 & 0 & 0 & 0 & 0 & \dfrac{\beta_{12}^A N_2^A}{\mu_v N_2} \\ \dfrac{\beta_{21}^C V_1\left(\gamma_2^C + \nu + \mu_2^C + m_{12}^C\right)}{N_1\left(D^C\right)} & \dfrac{\beta_{21}^C V_1 m_{12}^C}{N_1\left(D^C\right)} & \dfrac{\beta_{21}^A V_1\left(\gamma_2^A + \mu_2^A + m_{12}^A\right)}{N_1\left(D^A\right)} & \dfrac{\beta_{21}^A V_1 m_{12}^A}{N_1\left(D^A\right)} & 0 & 0 \\ \dfrac{\beta_{22}^C V_2 m_{21} C}{N_2\left(D^C\right)} & \dfrac{\beta_{22}^C V_2\left(\gamma_1^C + \nu + \mu_1^C + m_{21}^C\right)}{N_2\left(D^C\right)} & \dfrac{\beta_{22}^A V_2 m_{21}^A}{N_2\left(D^A\right)} & \dfrac{\beta_{22}^A V_2\left(\gamma_1^A + \mu_1^A + m_{21}^A\right)}{N_2\left(D^A\right)} & 0 & 0 \end{pmatrix}$$

where

$D^C = \left(\gamma_1^C + m_{21}^C\right)\left(\gamma_2^C + m_{12}^C\right) - m_{12}^C m_{21}^C$, $D^A = \left(\gamma_1^A + m_{21}^A\right)\left(\gamma_2^A + m_{12}^A\right) - m_{12}^A m_{21}^A$. To get the basic reproduction number we need to solve $\det\left|\lambda I - J\right|$ which is a $6\times 6$ matrix. Rewriting the matrix in the form

$$\Theta = \begin{pmatrix} 0I_4 & B \\ A & 0I_2 \end{pmatrix}.$$

The determinant of $\Theta$ is given by

$$\det\left(\Theta-\lambda I_6\right)=\begin{pmatrix}-\lambda I_4 & B\\ A & -\lambda I_2\end{pmatrix}=\lambda^4\begin{vmatrix}I_4 & -\frac{1}{\lambda}B\\ A & -\lambda I_2\end{vmatrix}=\lambda^4\begin{vmatrix}\begin{pmatrix}I_4 & 0\\ A & I_2\end{pmatrix}\begin{pmatrix}I_4 & -\frac{1}{\lambda}B\\ 0 & -\lambda I_2+\frac{1}{\lambda}AB\end{pmatrix}\end{vmatrix}.$$

Using the properties of determinants we have

$$\det\left(\Theta-\lambda I_6\right)=\lambda^4\det\left(-\lambda I_2+\frac{1}{\lambda}AB\right)=\lambda^2\det\left(AB-\lambda^2 I_2\right)=0.$$

We see after some calculation, that

$$\mathcal{R}_0^2=\frac{a_0+\sqrt{a_0^2-4a_1}}{2}$$

where

$$a_0=\left(A_{11}B_{11}+A_{13}B_{31}+A_{22}B_{22}+A_{24}B_{42}\right)$$

$$a_1=\left[\left(A_{11}B_{11}+A_{13}B_{31}\right)\left(A_{22}B_{22}+A_{24}B_{42}\right)\right]-\left[\left(A_{21}B_{11}+A_{23}B_{31}\right)\left(A_{12}B_{22}+A_{14}B_{42}\right)\right].$$

The expression for $\mathcal{R}_0^2$, is complex due to the large number of parameters involved, but from the expression of the matrices *A* and *B* above, we can gain some insight. For example if there is no human migration between the two patches, then $m_{12}^C=m_{21}^C=m_{12}^A=m_{21}^A=0$ and

$$\mathcal{R}_0^2=\frac{a_0+\sqrt{a_0^2-4a_1^*}}{2}$$

where

$$a_1^*=\left(A_{11}B_{11}+A_{13}B_{31}\right)\left(A_{22}B_{22}+A_{24}B_{42}\right).$$

This is the product of the maximum basic reproduction number for patch 1 and patch 2.

If there is no infective vectors in patch 2, and no vector migration, then $\beta_{12}^C=\beta_{12}^A=0$, and

$$\mathcal{R}_0^2=\frac{\beta_{11}^C\beta_{21}^C\left(\gamma_2+\tilde{\mu}_2^C+m_{12}^C\right)N_1^C}{N_1^2\left[\left(\gamma_1+m_{21}^C\right)\left(\gamma_2+m_{12}^C\right)-m_{21}^Cm_{12}^C\right]}+\frac{\beta_{11}^A\beta_{21}^A\left(\gamma_2+\mu_2^A\right)N_1^AV_1}{N_1^2\left[\left(\gamma_1^A+m_{21}^A\right)\left(\gamma_2^A+m_{12}^A\right)-m_{21}^Am_{12}^A\right]},$$

which is the total children and adult contribution to $\mathcal{R}_0^2$.

It is clear that this new value of the basic reproduction number highly depends on the migration rates of the two age groups. If we increase the migration rates then $\mathcal{R}_0^2$ increases.

Biologically, this implies that back and forth movement between the patches, would introduce malaria infection in an otherwise malaria free patch.

## 4. Simulation

In this section we obtain baseline values for two sites: the U-shaped valleys and V-shaped valleys. and use them to simulate equation 1, which is a compact form of equation 5 in [1]. For the human population in our model, we consider two patches, Umutete and Iguhu for the U-shaped valleys, and, Marani and Fort Tenan for the V-shaped valleys. From the study on the different ecosystems, the plateaus and the U-shaped valleys ecosystem have the characteristic, such that the results for the V-shaped valleys apply to the plateau ecosystem. This results from the fact that on the plateaus, the terraine is characterised by raised but flat topography with very little stag- nant water as the water darains down the rivers, to support breeding places for mosquitoes. The only notable differences is where there are large water bodies like dams and reservoirs. In these cases high mosquito population is likely to survive and hence increase malaria transmission and infection. Some suitable references for our values are [12]-[16].

Data for $N_1, N_2$, and $N_v$ was estimated to be 10000 people and we assume that the population is evenly distibuted to the two patches so that we have 5000 people on each patch (1500 children and 3500 adults for each

ecosystem). The mosquito population likewise was estimated to be 80,000 mosquitoes in the U-shaped valleys and 10,000 mosquitoes in the V-shaped valleys.

The summary of the parameter values used is given in **Table 1**.

### 4.1. The U-Shaped Valley Sites: Iguhu and Umutete, When $\mathcal{R}_0 = 5.36$

When the age structuring is considered, the dynamics of the host population in the U-shaped valleys is represented on **Figure 1**. When there is no age structuring, the dynamics for the U-shaped valleys are shown in **Figure 2**. If we consider the U-shaped and the V-shaped valleys as one epidemiological region representing Western Kenya, then the dynamics are represented by **Figure 3**. The disease in the age structured model fades out faster. The steady states also settle to the endemic equilibrium faster.

If there is no spatialization the values for the U-shaped valleys for both ecosystems has host population variation represented on **Figure 3**. The interaction between the patches raises infection rate, so that the disease persists in the total population, while it fades out fast when the patches are isolated.

### 4.2. The V-Shaped Valley Sites: Fort Tenan and Marani, $\mathcal{R}_0 = 1.67$

The dynamics of the model in the V-shaped valleys sites with age structure is given by **Figure 4**. When the age structuring is ignored the variation of the host population in the V-shaped valleys is represented by **Figure 5**.

## 5. Conclusions

Highland malaria in Western Kenya remains a source of mortality and morbidity. Concerned efforts have been put in place by the stakeholders to bring the disease under control with less than expected results. This study

**Table 1.** Parameter values and ranges for System 1 and Equation (5) in [1].

| Parameter | U-Shaped valleys | V-shaped valleys |
|---|---|---|
| $a^C$ | 0.52 | 0.42 |
| $a^A$ | 0.15 | 0.12 |
| $b_1^C$ | 0.011 | 0.08 |
| $b_1^A$ | 0.011 | 0.08 |
| $b_2^C$ | 0.048 | 0.24 |
| $b_2^A$ | 0.024 | 0.018 |
| $\mu_h^C$ | 0.079 | 0.059 |
| $\mu_h^A$ | 0.033 | 0.033 |
| $\mu_v$ | 0.033 | 0.033 |
| $\nu$ | 0.000283 | 0.000283 |
| $m_{12}^C$ | 0.08 | 0.08 |
| $m_{21}^C$ | 0.08 | 0.08 |
| $m_{12}^A$ | 0.5 | 0.5 |
| $m_{21}^A$ | 0.5 | 0.5 |
| $m_{12}^v$ | 0.02 | 0.02 |
| $m_{21}^v$ | 0.02 | 0.02 |
| $\gamma^C$ | 0.0035 | 0.0035 |
| $\gamma^A$ | 0.0035 | 0.0035 |
| $\Lambda_h$ | 0.04 | 0.04 |
| $\Lambda_v$ | 0.13 | 0.07 |
| $N^C$ | 1500 | 1500 |
| $N^A$ | 3500 | 3500 |

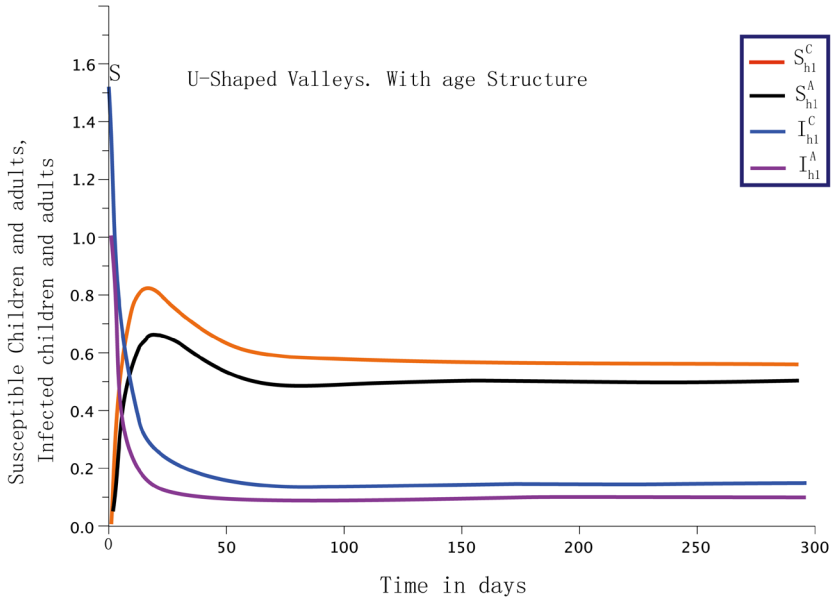


**Figure 1.** A numerical simulation for the variation of the two age classes population using Equation (1) and parameter values defined in **Table 1** for the U-shaped valleys system with $\mathcal{R}_0 = 5.36$.

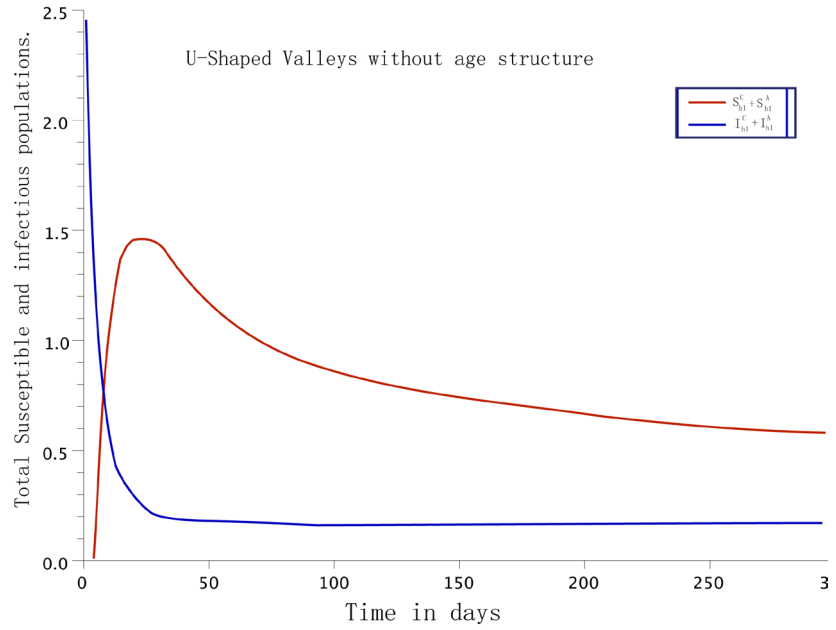


**Figure 2.** A numerical simulation of Equation (1) no age class in the population and $\mathcal{R}_0 = 5.36$.

captures important factors key to endemicity of of malaria in Western Kenya, which could direct control measure and targets effectively.

Age structure helps us differentiate between child's infectivity and susceptibility to malaria infection. It is clear from Balls [17] that children are a significant source of mosquito infection compared to adults. The biting rate for the two age groups differs [18] [19] as children are bitten more than adults did. The other difference captured in the model is death rates for the children (which may include malaria induced deaths). Most malaria deaths occur in children under the age of five years. While the adults also suffer morbidity due to severe in-

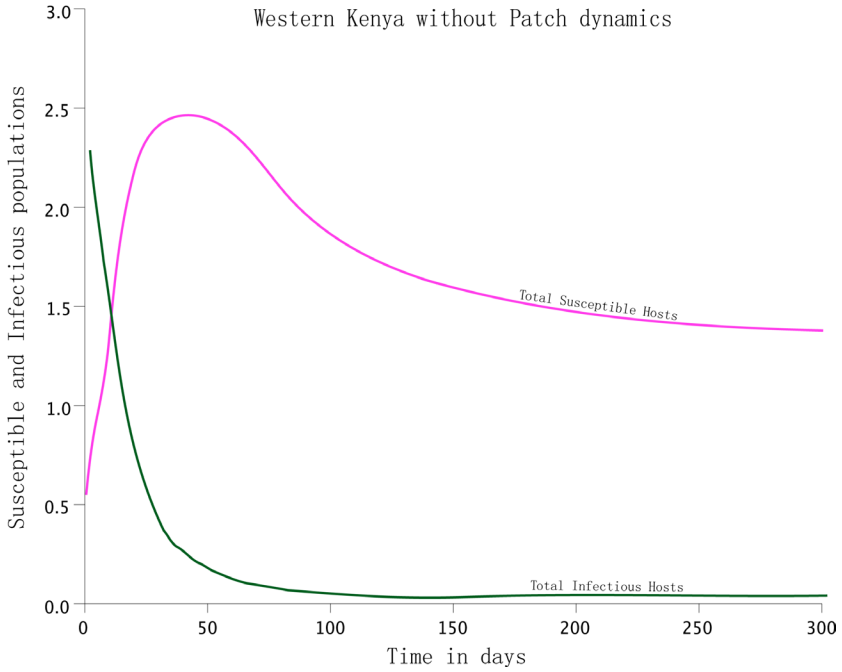


**Figure 3.** The variation of the total population in the region, no age class and the two ecosystems are treated as a single U-shaped valley ecosystem.

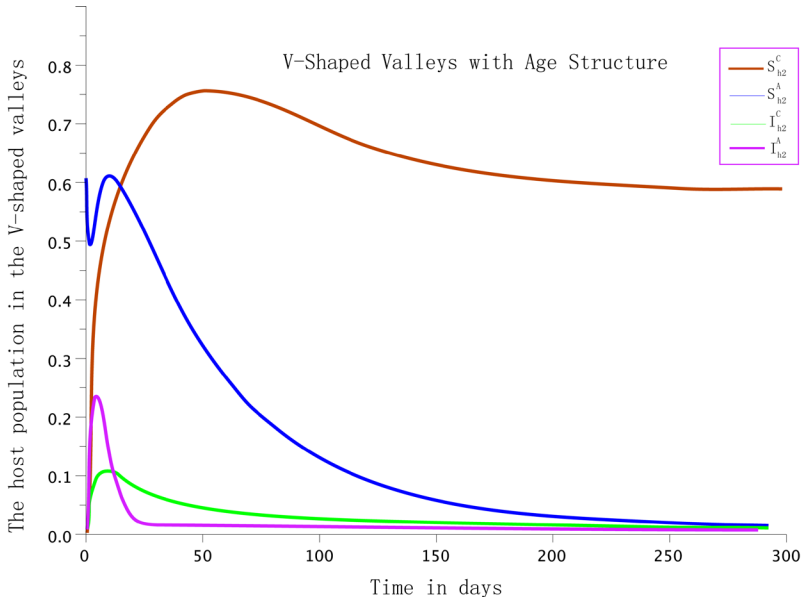


**Figure 4.** A numerical simulation of model 1 using parameter values defined in **Table 1** for the V-shaped valleys ecosystem with age structure. In this case $\mathcal{R}_0 = 0.96 < 1$.

fection of highland malaria, there are fewer deaths due to acquired immunity compared to children. We note that the populations settle to the endemic equilibrium faster than in the age-structured than in the unstructured system as shown in **Figure 5**, and the stable equilibrium is achieved faster in the structured than the unstructured system. Adding age structure allows age specific control strategies to reduce disease prevalence.

Our model suggests that a suitable model for malaria should be one that captures: age structure; differentiated patch or region susceptibility, which depends on the immunity of the inhabiting population; differentiated infectivity, which also depends on the immunity and age of the host population, and the mosquito population

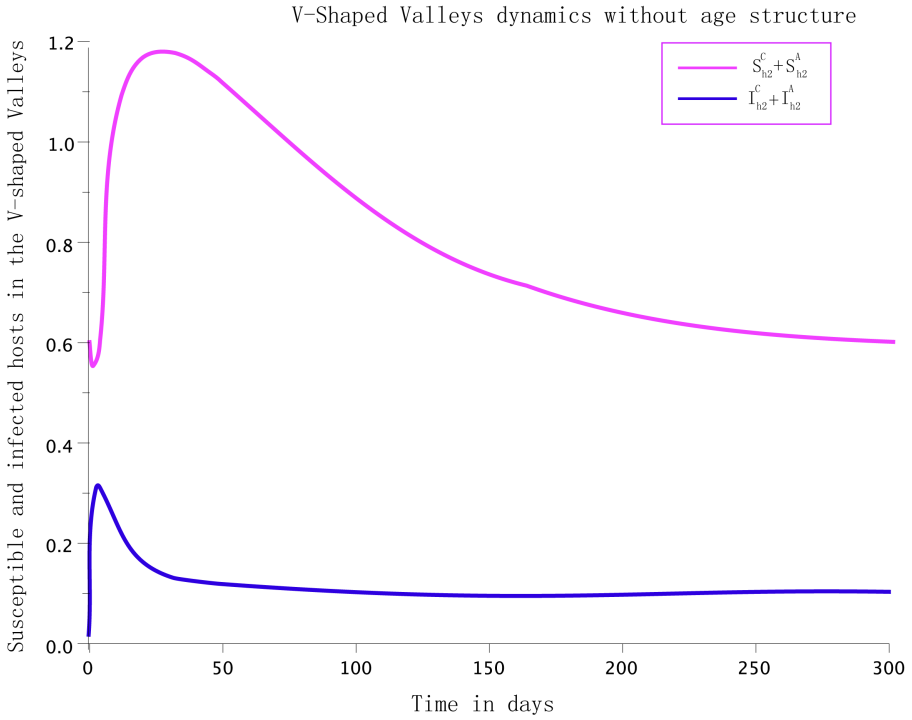


**Figure 5.** A numerical simulation of model 1 using parameter values defined in **Table 1** for the V-shaped valleys ecosystem without age structure. In this case $\mathcal{R}_0 = 0.96 < 1$, A numerical simulation of model 1 using parameter values defined in **Table 1** for the V-shaped valleys ecosystem. The is no age structures in the populations. In this case $\mathcal{R}_0 = 0.96 < 1$.

dynamics. Intervention then can be done with guidance from the model.

A more comprehensive characterization of results would have to include other types of patches that may not be terraine related but have different epidemiological characteristics from the U-shaped and the V-shaped valleys. Such patches could take care of cities like Nairobi, where human migration has transferred malaria, and central Kenya where the cool highland ecosystem is disturbed by creation of dams for irrigation, rice cultivation, climate change and migration of population to the economically endowed part of the county. Adding age structure allows age specific control strategies to reduce disease prevalence.

We assumed that vectors migrate especially to nearby patches, and the migration parameters for hosts are constant, similar and independent of the compartment. For the compartments that are far apart, the migration of mosquitoes is negligible and is set to zero, since the mosquitoes are only able to fly about 2 kilometers away.

An explicit formula for $\mathcal{R}_0$ is obtained, which although complex due to the infinite number of patches, can be used to explore the effects of the parameters of the model. This formula will allow theoretical exploration of the options and efficiency of targeted public health intervention policies. The example in the two ecosystems simplifies the expression for $\mathcal{R}_0$, which we use to simulate our model with some realistic data from Western Kenya. This parameter is inversely related to migration of the hosts between the patches. This implies that to reduce $\mathcal{R}_0^2$, we have to i) administer effective treatment through provision of proper health care facilities in both patches, ii) promote drug adherence, iii) reduce malaria drugs abuse through self administration to shorten the infectious period and arrest human to mosquito infection, hence increase the rate of recovery represented by $\gamma$.

An example in two patches is given with an expression of $\mathcal{R}_0$ which is still complex; but insight is given in a case when no migration takes place. If the disease exists in one patch, with the back and forth movement, the disease in the otherwise free patch would be reintroduced. We want to mention that an example in three patches is also possible, but meaningful insight for the basic reproduction number may only be gained by simulation, with relevant data. This model can be extended to include intervention strategies by the Ministry of health in Kenya, through ITNs and IRS. Since the disease causes death especially in children, the model can also include disease related death rate in the human population. An important factor which is under investigation is the im-

pact of climate related factors to the resurgent epidemics. Resistance of vectors to ITNs and IRS is also an important factor which may cause the disease to remain a menace in the region, not to mention the possibility of drugs resistance in human and possible emergence if new malaria strains.

So far, we have formulated an analytical and numerical analysis which is a foundation of more research and also applicable to other vector borne disease like chikungunya [20].

## Acknowledgements

We wish to acknowledge of the Inria Metz, UMMISCO(IRD), the French Embassy in Nairobi and the university of Nairobi, Kenya, for their financial, logistic and moral, support during the writing of this article. We are very grateful to Dr. Githeko, KEMRI Kisumu for the great insight and literature he gave us during this study.

## References

[1] Josephine, W.K., Gauthier, S. and Ogana, W. (2013) Formulation of a Vector SIS Malaria Model in a Patchy Environment with Two Age Classes. *Applied Mathematics*, **222**, 4444.

[2] Diekmann, O., Heesterbeek, J.A.P. and Metz, J.A.J. (1990) On the Definition and the Computation of the Basic Reproduction Ratio $R_0$ in Models for Infectious Diseases in Heterogeneous Populations. *Journal of Mathematical Biology*, **28**, 365-382. http://dx.doi.org/10.1007/BF00178324

[3] Diekmann, O. and Heesterbeek, J.A.P. (2000) Mathematical Epidemiology of Infectious Diseases in Mathematical and Computational Biology. Wiley Series, Hoboken.

[4] Van Den Driessche, P. and Watmough, J. (2002) Reproduction Numbers and Subthreshold Endemic Equilibria for Compartmental Models of Disease Transmission. *Mathematical Biosciences*, **180**, 29-48. http://dx.doi.org/10.1016/S0025-5564(02)00108-6

[5] Varga, R.S. (1962) Matrix Iterative Analysis. Prentice-Hall, Upper Saddle River.

[6] Thieme, H.R. (2009) Spectral Bound and Reproduction Number for Infinite-Dimensional Population Structure and Time-Heterogeneity. *SIAM Journal on Applied Mathematics*, **70**, 188-211. http://dx.doi.org/10.1137/080732870

[7] Varga, R.S. (1960) Factorisation and Normalised Iterative Methods Boundary Problems in Differential Equation. University of Wisconsin Press, Madison.

[8] La Salle, J.P. (1976) The Stability of Dynamical Systems. Society for Industrial and Applied Mathematics. Regional Conference Series in Applied Mathematics.

[9] Hirsch, M.W. (1982) Systems of Differential Equations that Are Competitive or Cooperative: I. Limit Sets. *SIAM Journal on Mathematical Analysis*, **13**, 167-179. http://dx.doi.org/10.1137/0513013

[10] Berman, A. and Plemmons, R.J. (1994) Nonnegative Matrices in the Mathematical Sciences, Volume 9 of Classics in Applied Mathematics. Society for Industrial and Applied Mathematics (SIAM), Philadelphia.

[11] Hirsch, H.W. and Smith, H.L. (2005) Monotone Dynamical Systems. In: *Handbook of Differential Equations*: *Ordinary Differential Equations*, Vol. II, Elsevier B. V., Amsterdam, 239-357.

[12] Chitnis, N., Hyman, J.M. and Cushing, J.M. (2008) Determining Important Parameters in the Spread of Malaria through the Sensitivity Analysis of a Mathematical Model. *Bulletin of Mathematical Biology*, **70**, 1272-1296. http://dx.doi.org/10.1007/s11538-008-9299-0

[13] Githeko, A.K., Branding-Bennet, D., Beier, M., Atieli, F., Owaga, M. and Collins, F.H. (1992) The Reservoir of Plasmodium Falciparum Malaria in a Holoendemic Area of Western Kenya. *Transactions of the Royal Society of Tropical Medicine and Hygiene*, **86**, 335-358.

[14] Ndenga, B., Githeko, A., Omukunda, E., Munyekenye, G., Atieli, H., Wamai, P., Mbogo, C., Minakawa, N., Zhou, G. and Yan, G. (2006) Population Dynamics of Malaria Vectors in Western Kenya Highlands. *Journal of Medical Entomology*, **43**, 200-206. http://dx.doi.org/10.1603/0022-2585(2006)043[0200:PDOMVI]2.0.CO;2

[15] UNICEF (2010) Kenya Statistics. Technical Report, United Nation, New York City.

[16] Wanjala, C.L., Waitumbi, J., Zhou, G. and Githeko, A.K. (2011) Identification of Malaria Transmission and Epidemic Hotspots in the Western Kenya Highlands: Its Application to Malaria Epidemic Prediction. *Parasites and Vectors*, **4**, 81. http://dx.doi.org/10.1186/1756-3305-4-81

[17] Balls, M.J., Bodker, R., Thomas, C.J., Kisinza, W., Msangeni, H.A. and Lindsay, S.W. (2004) Effect of Topography on the Risk of Malaria Infection in the Usambara Mountains, Tanzania. *Transactions of the Royal Society of Tropical Medicine and Hygiene*, **98**, 400-408.

[18] Mukabana, W.R., Takken, W., Richard, C. and Knols, B.G.J. (2002) Host-Specific Cues Cause Differential Attrac-

tiveness of Kenyan Men to the African Malaria Vector Anopheles Gambiae. *Malaria Journal*, **1**, 17. http://dx.doi.org/10.1186/1475-2875-1-17

[19] Smith, D.L., Guerra, C.A., Snow, R.W. and Simon, H.I. (2007) Standardizing Estimates of the *Plasmodium falciparum* Parasite Rate. *Malaria Journal*, **6**, 131. http://dx.doi.org/10.1186/1475-2875-6-131

[20] Bowong, S., Dumont, Y. and Tewa, J.J. (2013) A Patchy Model for Chikungunya-Like Diseases. *Biomath*, **2**, 1-19.

Scientific Research Publishing (SCIRP) is one of the largest Open Access journal publishers. It is currently publishing more than 200 open access, online, peer-reviewed journals covering a wide range of academic disciplines. SCIRP serves the worldwide academic communities and contributes to the progress and application of science with its publication.

Other selected journals from SCIRP are listed as below. Submit your manuscript to us via either submit@scirp.org or Online Submission Portal.